Iris Concavity, Corneal Biomechanics, and Their Correlations With Ocular Biometry in a Cohort of 10- to 12-Year-Old UK School Boys: Baseline Data

Ameet Shah,[1] Sancy Low,[1] David F. Garway-Heath,[1] Paul J. Foster,[1] and Keith Barton[1,2]

[1]National Institute for Health Research (NIHR) Biomedical Research Centre at Moorfields Eye Hospital National Health Service (NHS) Foundation Trust and University College London (UCL) Institute of Ophthalmology, London, United Kingdom
[2]Department of Epidemiology and Genetics, Institute of Ophthalmology, London, United Kingdom

Correspondence: Ameet Shah, UCL Institute of Ophthalmology, 11-43 Bath Street, London EC1V 9EL, UK; ameetshah001@gmail.com.

Submitted: December 11, 2013
Accepted: April 6, 2014

Citation: Shah A, Low S, Garway-Heath DF, Foster PJ, Barton K. Iris concavity, corneal biomechanics, and their correlations with ocular biometry in a cohort of 10- to 12-year-old UK school boys: baseline data. *Invest Ophthalmol Vis Sci*. 2014;55:3303–3310. DOI:10.1167/iovs.13-13756

Purpose. Pigment dispersion syndrome is associated with iris concavity. This study investigated the prevalence of iris concavity, defined as a measurement of ≤ -0.1 mm, in a cohort of 10- to 12-year-old boys, and explored the relationship between iris curvature and anterior segment biometry. Associations with corneal biomechanical parameters also were explored.

Methods. A cohort of school boys ($n = 96$) was recruited from a local school. Anterior segment optical coherence tomography (AS-OCT) was performed under accommodative and nonaccommodative conditions, and iris curvature quantified. Corneal hysteresis (CH) and corneal resistance factor (CRF) were measured with the ocular response analyzer (ORA). Noncontact axial biometry was performed using laser interferometry.

Results. The prevalence of iris concavity was 24% on distance fixation, increasing to 65% on accommodation. Variables significantly associated with nonaccommodating iris curvature were lens vault ($P = 0.02$) and mean keratometry ($P = 0.02$). For both variables acting jointly, $R^2 = 0.30$. Variables associated significantly with accommodating iris curvature were anterior chamber depth ($P = 0.009$), lens vault ($P = 0.049$), and mean scleral spur angle ($P < 0.0001$). For these three variables acting jointly, $R^2 = 0.33$. Significant association was found between CH and spur-to-spur distance ($R^2 = 0.07$, $P = 0.025$).

Conclusions. Iris concavity was a common finding in this cohort and related to anterior segment biometric parameters. Further work is required to clarify whether anatomical differences exist between iris concavity seen in the adolescent eye and that found in adults with pigment dispersion syndrome.

Keywords: anterior segment optical coherence tomography, iris concavity, pigment dispersion, corneal hysteresis, refractive error

Iris concavity has been implicated in the pathogenesis of pigment dispersion syndrome (PDS): the concept of the "reverse pupillary block" mechanism was introduced by Karickoff,[1] who proposed that abnormal iridolenticular contact during accommodation causes the iris to act like a flap valve, permitting unidirectional flow of aqueous from the posterior to the anterior chamber. The relative reduction in pressure in the posterior chamber postulated to occur during accommodation, therefore, is prevented from equalizing with the anterior chamber, resulting in posterior bowing of the midperipheral iris. Campbell[2] proposed that frictional contact between packets of anterior zonular fibers and the posterior pigment epithelium resulted in pigment dispersion. Physiologic iris concavity also has been observed in normal subjects in the resting state[3] and following exercise,[4] but its prevalence during eye growth in normal subjects is not well known. The tendency to iris concavity is more pronounced in myopic eyes,[4] but its relationship with other ocular biometric parameters has not been studied to date to our knowledge.

The incidence of myopia is increasing, and several large studies from the United States and Far East Asia have provided data in school age children. The Singapore Cohort study of the risk factors for myopia (SCORM)[5] found that 34% of 7- to 9-year-olds were myopic at baseline, while a large US study report only 10% of a slightly older cohort (mean age 10 years) were myopic.[6] There are relatively little contemporary data on the UK prevalence/incidence of myopia in young people. Williams et al.[7] reported a prevalence of spherical equivalent (SE) < -1.5 diopters (D) of 1.5% in 7-year-olds from autorefraction data in a cohort of children in the Avon area, Southwest England. This figure increased to 3.6% when the same cohort was re-examined 3 years later.

A number of easily measurable quantitative traits have been identified using noncontact devices and are considered to be important determinants of refractive error.[8] Hussin et al.[9] report on the accuracy of AL measurements made by the IOLMaster (Carl Zeiss Meditec Ltd., Welwyn Garden City, UK) with ultrasound A-scan in a pediatric cohort (mean age, 11.4 years) and found no statistically significant difference between the two methods. A study in Japanese 7- to 13-year-old myopes demonstrated the ability of the IOLMaster to provide highly repeatable axial length (AL) measurements in this age group.[10]

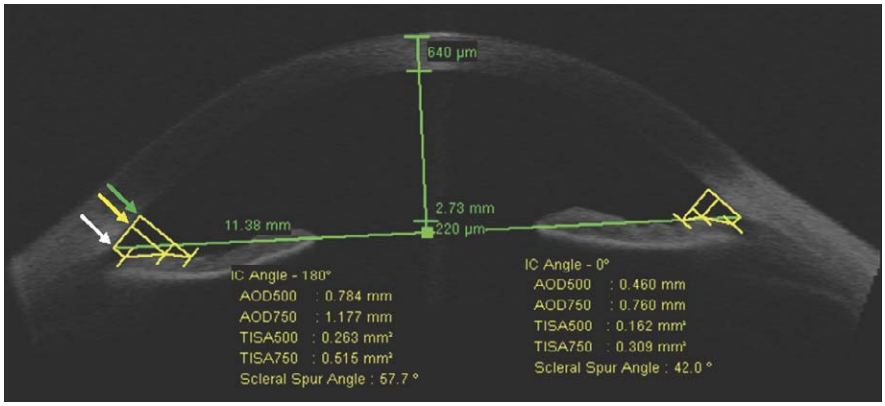

Figure 1. Example AS-OCT screenshot demonstrating measurements. *White arrow* denotes scleral spur. *Yellow* and *green arrows* denote points 500 and 750 µm, respectively, anterior to scleral spur along corneal endothelium.

There is some evidence that corneal biomechanical properties may be related to axial biometry. Corneal hysteresis (CH), a parameter considered to represent the dampening or viscoelastic properties of the cornea,[11] was lower in eyes with longer AL in a study by Song et al.[12] on 1153 secondary school children in rural China. However, a cross-sectional study of 271 Singaporean children,[13] reporting on CH and the "corneal resistance factor" (CRF), did not show any association with refractive error or axial length.

The primary aim of this study was to estimate the prevalence of iris concavity in 10- to 12-year-old UK boys in the accommodative and nonaccommodative states. Anterior chamber biometric parameters were measured and the correlation between iris concavity, and AL, SE, CH, and CRF were investigated. We described the study design and baseline data. Longitudinal data from the same cohort, remeasured 2 years later, will be published in a separate report.

Methods

Eligibility and Recruitment

All students in two consecutive year groups at City of London School were considered eligible for enrolment. The study was approved by the Moorfields and Whittington Research Ethics Committee. This study adhered to the tenets of the Declaration of Helsinki.

Following logistic arrangements with the school, and an introductory lecture to the students, information sheets and consent forms were sent to all of the students and their parents.

Of 140 boys invited to take part, 103 (73.6%) returned registration forms indicating a willingness to participate and 96 (68.6%) attended on the day. One eye of each participant was preselected at random using a web-based research randomization tool[14] and this eye was designated as the study eye.

Examination and Imaging

Visual Acuity. Distance visual acuity was measured in each eye at 4 meters with their current spectacles if available. (LogMAR Acuity Charts; Keeler Ltd., Windsor, UK). Pinhole visual acuity also was measured if the initial visual acuity was logMAR 0.2 (Snellen equivalent 20/32) or worse.

Assessment of Ocular Refraction. Noncycloplegic ocular refraction was measured using an autorefractor (Nvision-K5001; Shin-Nippon Commerce, Inc., Tokyo, Japan). The room in which the study was conducted overlooked the Thames river and the autorefractor was set up such that the subject fixated on a designated target on a building on the opposite bank of the river to minimize accommodation. Manual focimetry was performed where spectacles were worn.

Ocular Biometry. The AL of the study eye was measured using laser interferometry (IOLMaster; Carl Zeiss Meditec Ltd.). The subject was asked to focus on the internal fixation target and the reflection of the alignment light was centered within the cross hairs on screen. A minimum of 5 measurements was taken and checked for consistency, paying attention to any software notifications indicating measurements requiring evaluation. Only measurements within 0.1 mm of each other were included in calculating mean AL. Readings with a signal-to-noise ratio of <2.0 were excluded.

Corneal Biomechanical Properties. The Ocular Response Analyzer (ORA; Reichert, Inc., Depew, NY, USA) measures the corneal response to indentation by a rapid air pulse, and derives values for CH and CRF.[11,15] The device also uses corneal biomechanical data to generate corneal-compensated IOP (ccIOP), a measure of IOP that is less affected by corneal properties.[16] The device was used to obtain at least three good quality measurements as determined by visual inspection of the waveform looking for sharp, well-defined raw signal peaks. The ORA software generates a waveform score reflecting measurement quality. Only measurements with a waveform score of ≥ 4 were included in the analysis.

Anterior Segment Optical Coherence Tomography (AS-OCT). Images of the anterior segment were obtained using the Visante AS-OCT (Carl Zeiss Meditec Ltd.). The device uses an internal fixation device with the apparent viewing distance set to infinity by the instrument optics when the subject's refraction is entered. The operator can stimulate accommodation by adjusting the focus of the internal fixation target.

Image Acquisition. The AS-OCT imaging was performed using near and distance fixation targets switching room lights off before image acquisition to minimize pupil constriction, and associated iris stretch, thereby maximizing iris curvature. The subject was instructed to look at the asterisk, which was the internal fixation target. The operator then aligned the eye using the video feedback window in the lower left corner of the display. The white dot in the center of the pupil represents the red reflex. Clicking on this dot centered the eye on the *x*- and *y*-axes. The *z*-axis was aligned by scrolling the mouse wheel forwards or backwards, which controlled the position of the chin- and head-rest relative to the device. Fixation was monitored using the video-feedback screen and the appearance of a central interference flare was used to indicate good

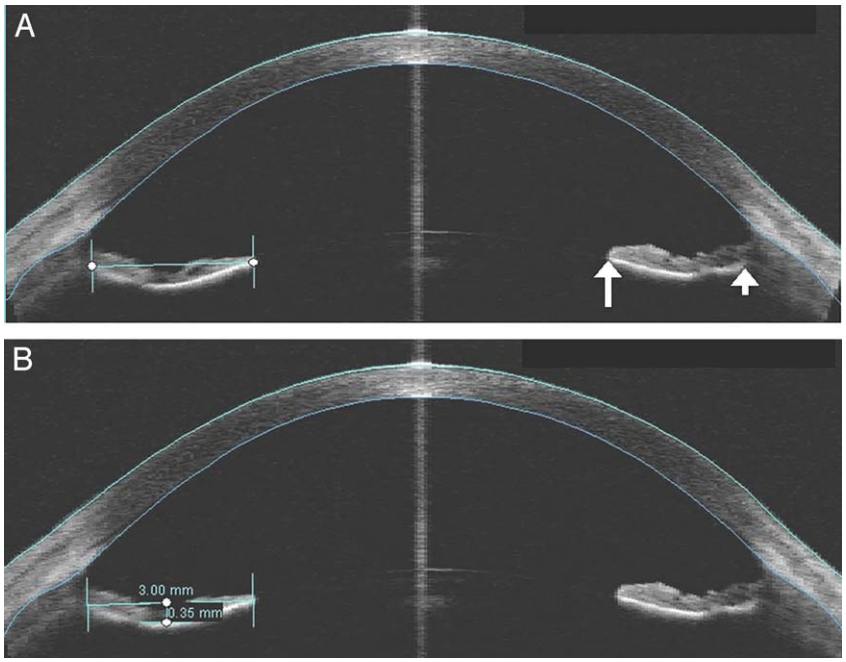

FIGURE 2. Iris curvature quantification. (**A**) A single caliper marking the posterior iris pigment epithelium at the pupil margin (*long arrow*) to ciliary sulcus (*short arrow*) was constructed (caliper shown on opposite quadrant for clarity). (**B**) At the point of maximum iris deflection, a second caliper was placed perpendicular to the first caliper shown in (**A**). The reading from this was used to determine the iris curvature. Negative values were observed for concave irides and positive values for convex irides. In this example, iris curvature is recorded as –0.35 mm.

centration. A scan of the temporal and nasal quadrants was taken using the "horizontal scan" protocol. As the focimetry/autorefraction details had been entered during the registration process, this scan was deemed to represent the nonaccommodating state.

The "POWER" tab, which controls the focus of the fixation target and is set by default to zero, was reduced gradually while asking the subject if he still could see a clear and sharp image. The value at which the child reported a blurred image was noted (e.g., –10.00 D). The child was moved away and the power value determined above was exceeded (e.g., –11.00 D) before placing the subject back onto the chin rest. The power value then was made gradually more positive, acquiring the image once the child reported seeing a sharp image again (e.g., –9.75 D). This second scan was deemed to represent near fixation.

Image Processing. The AS-OCT images were analyzed using the device's Visante 3.0 software by one investigator (AS); accommodative and nonaccommodative images were analyzed. The scleral spur was defined as the point where there was a change in curvature of the inner surface of the angle wall, usually marked by an inwards protrusion of the sclera.[17] The scleral spur and anterior surface of the lens were identified by the operator, and based on these landmarks, the software calculated the following parameters (Fig. 1): anterior chamber depth (ACD), lens vault (LV), central corneal thickness (CCT), angle opening distances (AOD) at 500 and 750 μm from scleral spur (AOD500 and AOD750), and trabecular-iris space area (TISA) at 500 and 750 μm from the scleral spur (TISA500 and TISA750). The AOD500 and AOD750 represent the perpendicular distances from the points 500 and 750 μm, respectively, anterior to the scleral spur to the anterior iris surface (Fig. 1).[18] The TISA500 and TISA750 represent areas bordered anteriorly by AOD500 and AOD750, respectively, posteriorly by a line from the scleral spur, parallel with the AOD to the anterior iris surface, superiorly by the inner corneal wall and inferiorly by the anterior iris surface.[19] The LV is defined as the perpendicular distance between the anterior pole of the crystalline lens and the horizontal line joining the scleral spur at the 9 and 3 o'clock positions, on horizontal AS-OCT scans. In addition, iris curvature was calculated using the software's caliper tool. The key anatomical landmark was the posterior pigment epithelium of the iris, which is seen as a well defined line of increased signal reflectance running on the posterior iris surface from the pupil margin to the iris root. Iris curvature was calculated as follows: A line was constructed from the innermost to the outermost extremity of the posterior pigment epithelium (Fig. 2A). The point along this straight line where iris was maximally deflected was identified and a second line, perpendicular to the first, was constructed from this point to the iris pigment epithelium (Fig. 2B). The length of this line was recorded as the iris curvature.[20] The measurement was assigned a negative value if the iris was concave and a positive value if convex. For the purposes of this study, iris concavity was defined as a measurement of $\leq$–0.1 mm.

Agreement of AS-OCT iris curvature measurements has been investigated previously: 95% confidence intervals (CIs) for limits of agreement were –0.07 to 0.05 mm between observers and –0.06 to 0.07 mm within observer (Shah A, et al. *IOVS* 2010;51:ARVO E-Abstract 5539). Between-observer agreement of semiautomated anterior segment parameters was assessed by randomly selecting 20 subjects for assessment by an experienced investigator (SL).

TABLE 1. Baseline Ocular Characteristics

Parameter	Mean	SD
SE, D	–0.33	1.7
AL, mm	23.80	0.95
CH, mm Hg	11.8	1.7
CRF, mm Hg	11.9	1.8
Corneal-compensated IOP, mm Hg	15.5	4.3

Table 2. Between-Observer Agreement on AS-OCT Parameters on 40 Images (Accommodative and Nonaccommodative Scans) From 20 Randomly Selected Subjects

Parameter	Range	Mean Difference	95% Limits of Agreement
CCT, μm	440 to 650	−1.8	−18.3 to +14.8
ACD, mm	2.44 to 4.00	0.01	−0.08 to +0.09
Lens vault, μm	−560 to 770	41.5	−93.3 to +176.3
Temporal AOD 500, μm	0 to 2016	−120	−380 to +150
Temporal AOD 750, μm	0 to 2245	−120	−390 to +160
Temporal TISA 500, mm²	0 to 0.837	−0.04	−0.13 to +0.05
Temporal TISA 750, mm²	0 to 1.357	−0.07	−0.21 to +0.08
Temporal scleral spur angle, deg	20.9 to 79.3	−3.9	−12.6 to +4.9
Spur-to-spur distance, mm	10.29 to 13.10	0.07	−0.1 to +0.24
Nasal AOD 500, μm	0 to 1698	−80	−370 to +210
Nasal AOD 750, μm	0 to 2170	−80	−420 to +250
Nasal TISA 500, mm²	0 to 0.568	−0.02	−0.13 to +0.08
Nasal TISA 750, mm²	0 to 1.063	−0.05	−0.22 to +0.13
Nasal scleral spur angle, deg	29.1 to 76.6	−2.7	−11.6 to +6.2

Statistical Analysis

To determine which variables were associated with iris curvature (as a continuous variable), multiple regression analysis was performed using 7 variables (spur-to-spur distance, ACD, LV, mean scleral spur angle, mean corneal curvature, SE, and AL). Linear regression analysis was used to investigate the relationship between AL/spur-to-spur distance and CH/CRF (dependent variable). Bland-Altman plots were constructed to assess between-observer agreement of AS-OCT parameters; the difference between observers and the magnitude of the parameter being measured was assessed for trend by linear regression analysis. The 95% limits of agreement (LoA) were calculated as appropriate. Analyses were performed using Prism version 6.0c for Mac OS X (GraphPad Software, La Jolla, CA, USA) available in the public domain at www.graphpad.com and MedCalc for Windows, version 12.2.1.0 (MedCalc Software, Mariakerke, Belgium).

Results

We examined 96 boys aged 11.51 ± 0.5 (mean ± SD) years. Seven participants exited the testing circuit early in error and did not attend the AS-OCT station. The Visante image in accommodation from one participant showed marked ghosting and was excluded from the analysis. A total of 79 subjects had at least 1 set of adequate quality ORA measurements. Summary data for age, AL, SE, CH, CRF, and IOPcc are shown in Table 1. All parameters were distributed normally as determined by the Kolmogorov-Smirnov test except for SE.

In the Bland Altman plots, the measurement difference between observers was unrelated to the magnitude of the measurement for all parameters. The 95% LoA together with the range of values in this cohort are shown in Table 2. The criterion for minimum acceptable LoA is a clinical decision, judged against the distribution of values (range).[21] The CCT, ACD, and spur-to-spur distance demonstrated reasonably good agreement; lens vault, scleral spur angle, and all AOD and TISA measurements demonstrated moderate agreement when considered in the context of the range of values for these parameters. Interestingly, ACD and spur-to-spur distance were operator-determined, but showed better agreement than the angle metrics that were software-determined.

A total of 25 boys had focimetry measurements and autorefraction measurements performed. In this group, right eye mean SE measured by focimetry was −1.76 D compared to −2.16 D by autorefractor ($P = 0.003$, paired t-test). Equivalent values of left eye were −2.26 D by focimetry compared to −2.21 D by autorefractor ($P = 0.78$).

The AS-OCT measurements at near and distance fixation are shown in Table 3. Using a cutoff of iris curvature ≤ −0.1 mm to define iris concavity, the prevalence of iris concavity in the nonaccommodative state was 24% and on accommodation it was 65% (Cochran's $Q = 33.0$, $P < 0.001$). The effect of changing this cut-off on prevalence values is shown in Table 4. Multiple regression analysis revealed the only variables

Table 3. Summary Data for AS-OCT Parameters

	Nonaccommodating, $n = 89$		Accommodating, $n = 88$		
Parameter	Mean	SD	Mean	SD	P*
Iris curvature, mm	−0.002	0.12	−0.21	0.18	<0.0001
CCT, μm	531.8	34.0	530.7	36.4	0.52
ACD, mm	3.34	0.27	3.11	0.31	<0.0001
Lens vault, μm	−171.5	190.9	46.9	259.0	<0.0001
Temporal AOD 500, μm	851.0	312.1	933.0	331.6	0.0034
Temporal TISA 500, mm²	0.303	0.117	0.321	0.124	0.24
Temporal scleral spur angle, deg	56.9	10.4	59.5	9.3	0.0023
Nasal AOD 500, μm	806.6	295.4	895.7	334.3	0.0008
Nasal TISA 500, mm²	0.275	0.099	0.294	0.108	0.03
Nasal scleral spur angle, deg	56.3	9.8	58.8	9.9	0.0043
Spur to spur distance, mm	11.99	0.47	11.96	0.48	0.69

* Paired t-test.

TABLE 4. Prevalence of Iris Concavity According to Iris Curvature Cutoff Used

Iris Curvature Cutoff, mm	Prevalence Nonaccommodating, %	Prevalence Accommodating, %
≤−0.1	24	65
≤−0.2	8	61
≤−0.3	2	30
≤−0.4	0	13
≤−0.5	0	5

significantly associated with nonaccommodating iris curvature were lens vault ($t = 2.43$, $P = 0.02$) and mean keratometry ($t = -2.38$, $P = 0.02$). For these two variables acting jointly, $R^2 = 0.30$. A scatterplot of lens vault against nonaccommodating iris curvature is shown in Figure 3. Variables significantly associated with accommodating iris curvature were ACD ($t = 2.68$, $P = 0.009$), lens vault ($t = -2.00$, $P = 0.049$), and scleral spur angle ($t = -5.0$, $P < 0.0001$). For these three variables acting jointly, $R^2 = 0.33$. A scatterplot of scleral spur angle against accommodating iris curvature is shown in Figure 4.

The CH and CRF were associated with spur-to-spur distance in the nonaccommodating state ($R^2 = 0.07$ for both, $P = 0.025$ and 0.027, respectively). The CH (but not CRF) was associated with spur-to-spur distance in accommodation ($R^2 = 0.11$, $P = 0.005$). A scatterplot of corneal hysteresis against spur-to-spur distance is shown in Figure 5. No significant association was found between CH/CRF and AL.

There were statistically significant differences between near and distance measurements for all angle metrics except temporal TISA500 ($P = 0.09$). Mean anterior lens surface movement on accommodation was 0.23 mm (SD 0.17 mm).

A total of 14 participants had an uncorrected refractive error (defined as visual acuity of logMAR 0.2 or worse which improved with pinhole). Letters were written to the parents of these participants advising them of the need for an optometric assessment. One was subsequently diagnosed as having keratoconus. Ten had ORA IOPcc values of greater than 21 mm Hg and were offered appointments in a Pediatric Ophthalmology clinic. One was noted to have significant angle recession secondary to a prior ocular injury.

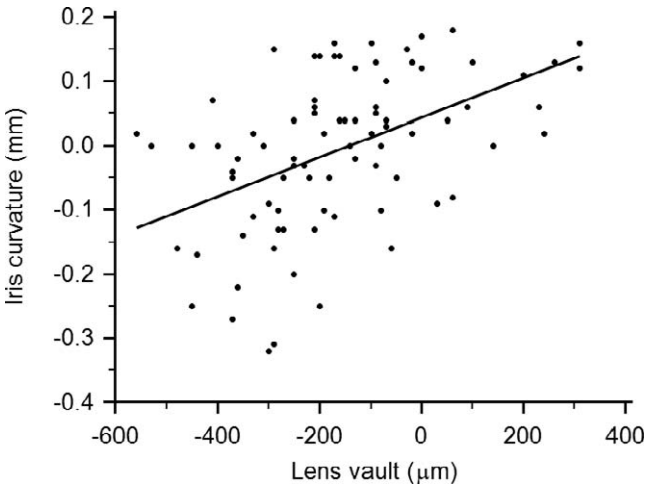

FIGURE 3. Scatterplot of lens vault against iris curvature (nonaccommodating). Regression equation: $y = 0.0003x + 0.04$.

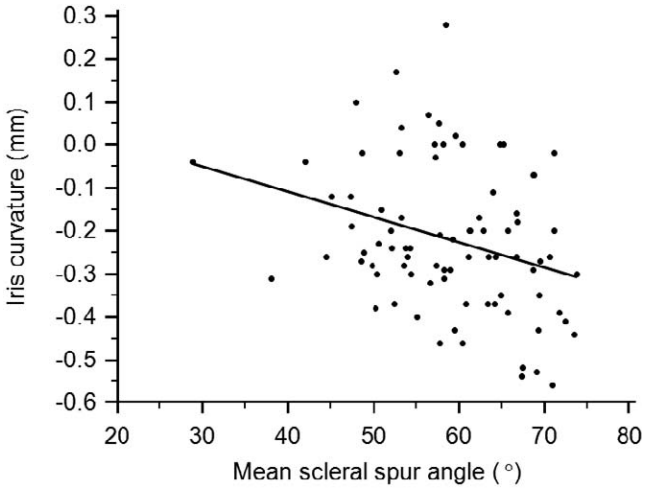

FIGURE 4. Scatterplot of mean scleral spur angle against iris curvature (accommodating). Regression equation: $y = -0.006x + 0.120$.

DISCUSSION

Iris concavity in PDS leads to increased frictional contact between the posterior iris surface and the lens zonules, thereby predisposing to pigmentary glaucoma. Iris concavity in the absence of PDS has been described (Ref. 3 and Laemmer R, et al. *IOVS* 2008;49:ARVO E-Abstract 5072), but its prevalence has not been reported. As PDS is a condition that often affects young males, this study was designed to look at the prevalence of iris concavity in a cohort of males before the age at which PDS typically is identified.

A more concave nonaccommodative iris profile was associated with a more negative lens vault, that is, a more posterior relative lens position. The reason for this may be that a relatively posterior lens position provides more space for the midperipheral iris to be displaced backwards.

Iris concavity was significantly more prevalent during accommodation than with distance fixation. The most widely accepted theory of accommodation is that put forward by Helmholtz,[22] which states that contraction of the ciliary muscle relaxes the tension in the lens zonules which allows the lens to revert to a thicker and more convex form. Drexler

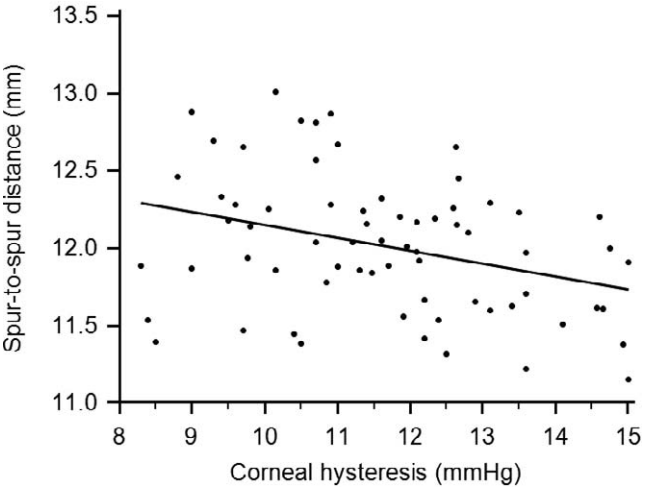

FIGURE 5. Scatterplot of corneal hysteresis against spur-to-spur distance (accommodating). Regression equation: $y = -0.08x + 13.0$.

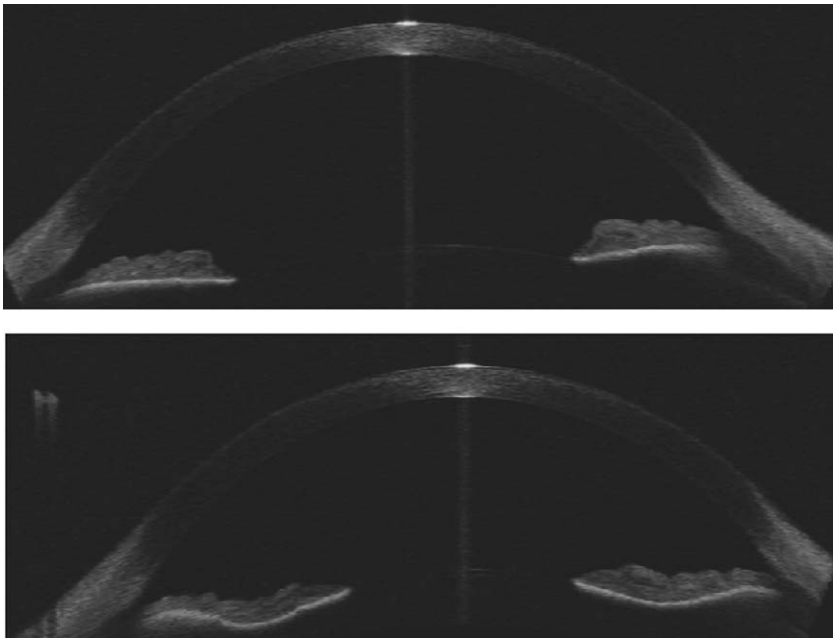

FIGURE 6. Example AS-OCT image showing convex iris curvature at distance fixation (*upper image*) and concave iris curvature in the same eye at near fixation (*lower picture*).

et al.[23] studied changes in lens position in 10 healthy eyes whose refractive error ranged from emmetropia to −5 D using partial coherence interferometry. During accommodation the mean forward movement ± SD of the anterior pole of the lens was 185 ± 89 μm (mean value 230 μm in the present study) while the backwards movement of the posterior pole was 69 ± 39 μm. Sheppard et al.[24] demonstrated a decrease in anterior and posterior radius of curvature during accommodation in 15 young (19–29 years) emmetropes using magnetic resonance imaging as well as an increase in lens thickness and decrease in AC depth. Visual inspection of the images from our cohort suggests that the central iris may be conforming to the curvature of the lens as it moves anteriorly (Figs. 6, 7). The parameter most strongly associated with iris concavity in accommodation was ACD. This also would support the hypothesis of anterior lens movement causing increased iris concavity. However, if miosis and forward movement of the anterior lens pole are the only conformational change, this would cause a reduction in the anterior chamber angle, AOD, and TISA on accommodation, rather than the increase observed (Table 2). As there appear to be accommodation-induced changes in the peripheral iris, it is unlikely that the changes seen in iris curvature are explained solely by anterior lens movement acting on the central iris. Accommodation-

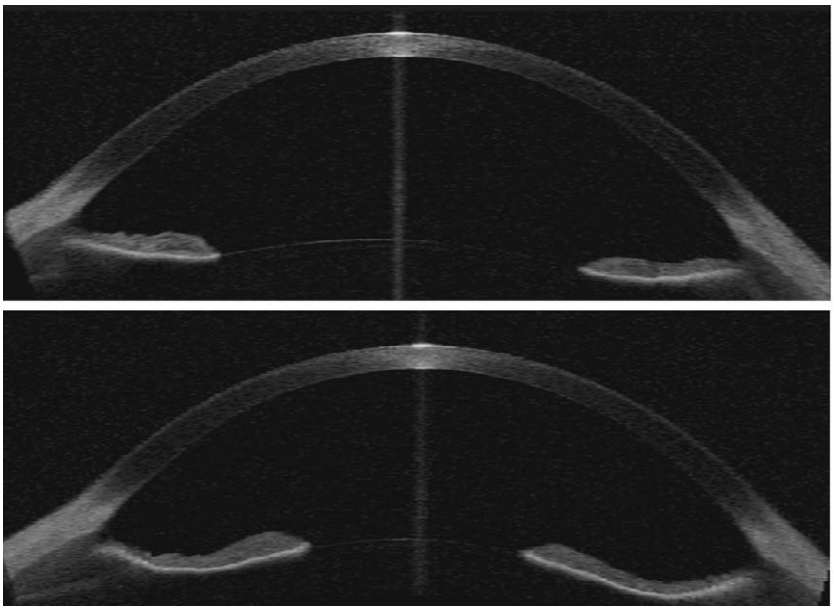

FIGURE 7. Example AS-OCT image showing a slightly concave iris curvature on distance fixation (*upper image*) with a marked increase in iris concavity in the same eye on near fixation (*lower picture*).

induced change in lens position and miosis are likely to increase the area of contact between the iris and lens, and this may result in a reverse pupillary block effect, similar to that seen in PDS, permitting mainly unidirectional flow from the posterior to the anterior chamber. The consequent increase in pressure in the anterior chamber relative to the posterior chamber may result in posterior displacement of the peripheral iris. This is a possible explanation for the increase in angle parameters seen on accommodation.

Multiple regression analysis also identified corneal curvature as being significantly associated with iris curvature at distance. One study has reported that patients with pigment dispersion have flatter corneas by approximately 2 D compared to age- and refraction-matched controls.[25] Yip et al.[26] investigated interocular differences in eyes with PDS and identified a flatter curvature of the posterior corneal surface to be associated with greater pigment loss. They hypothesize that flatter corneas are biomechanically less resistant to the pressure of the eyelids, causing aqueous to be pushed backwards against the iris, thereby potentiating iris concavity.

Of the eyes, 24% exhibited iris concavity in the nonaccommodative state. As the prevalence of PDS in a white population reportedly is 2.5%,[27] the vast majority of these eyes are unlikely to develop PDS. It may be that iris concavity and the associated iridolenticular contact must persist into adulthood for the development of PDS or other features must be present to induce pigment dispersion, such as factors intrinsic to the iris of PDS patients causing susceptibility to zonular abrasion or pigment shedding.

Good between- and within-observer agreement of the iris concavity measurements used in this study has been previously shown in a cohort of adult PDS patients (Shah A, et al. *IOVS* 2010;51:ARVO E-Abstract 5539). We conducted our own between-observer agreement study on the semiautomated AS-OCT parameters. Imperfect agreement may be due to differences in scleral spur identification, as well as the effect of automated iris surface detection. Liu et al.[28] reported that scleral spur identification is more difficult in eyes with narrow angles. In general, scleral spur visibility was good in the vast majority of images it this study. This was supported by better agreement for scleral spur angle and spur-to-spur distance, whereas agreement for the automated readings for AOD and TISA were less good.

The CH, CRF, and IOP measured by the ORA have been described previously.[11] Kirwan et al.[29] report noncontact tonometry with the ORA to be an accurate method of determining IOP and found children cooperated better with this technique than with Goldmann applanation tonometry. Lower CH has been associated with longer AL in Chinese school children[12,30] although Lim et al.[13] did not find any association with AL or refractive error in their study of 271 Singaporean (68.6% Chinese) children. Chang et al.[31] studied 126 eyes of 63 Taiwanese (predominantly Han Chinese) children and found that the difference in CH between the two eyes of each patient correlated significantly with the difference in the AL between the two eyes. There was no relationship between ORA measurements and AL in the present study. Any potential relationship may have been confounded by the ethnically mixed nature of our cohort. However, there were statistically significant relationships between CH/CRF and spur-to-spur distance, which may be regarded as a correlate of eye size. The CH is a measure of the energy absorption during the loading/unloading of the stress–strain cycle of viscoelastic materials.[32] Huang et al.[30] conducted a retrospective review of 1020 patients and report that CH was associated with corneal volume (regression coefficient = 0.059, $P = 0.014$). The positive association with spur-to-spur distance in the present study, and corneal volume in the study by Hwang et al.[33] are in keeping with CH being a measure of energy absorption as both parameters are correlates of anterior segment size and a larger anterior segment may better absorb energy. Interestingly, CH was found to correlate significantly with superior and inferior angle width in a recent study reporting on 17 eyes with pigmentary glaucoma.[34] Our second report of the 2-year follow-up of this cohort investigated whether these correlations remained significant over time.

Children in this age group have a large amplitude of accommodation and the autorefractor may have overestimated the degree of myopia, given that eyes were not cyclopleged. Entering this refraction value into the AS-OCT may have induced accommodation unintentionally. Results from 25 subjects revealed that on average autorefraction overestimated myopia by only 0.4 D compared to focimetry in the right eye, while no significant difference was found in the left eye. However, even using the focimetry refraction may not fully relax accommodation, as "the full plus" is not always prescribed in this age group.

A further limitation is the study did not look at females of the same age group. While pigmentary glaucoma is more common in men,[35–37] the prevalence of pigment dispersion syndrome is similar in men and women.[35,38] The PDS is seen rarely in children, although Doroiraj et al.[39] describe an 11-year-old girl and two 12-year-old boys with PDS and raised IOP. Thus, it would have been interesting to study a female cohort in the same age group to investigate the prevalence of iris concavity.

In conclusion, we reported a high prevalence of iris concavity in this cohort of 10- to 12-year-old boys. Iris curvature was associated with LV in the nonaccommodated state and with ACD, LV, and scleral spur angle in the accommodated state. It remains unclear whether there may be anatomical differences between the type of iris concavity found in our cohort and that found in PDS, and this remains an area for further study. Our data supported the hypothesis that physiologic iris concavity, which is more prominent during accommodation may be related to a reverse pupil block mechanism. The anterior movement of the central iris alone did not explain the wider angle metrics and observed changes in iris curvature. Our study also suggested there may be significant associations between corneal biomechanical parameters and ocular size (determined by spur-to-spur distance but not AL in this dataset).

Acknowledgments

The authors thank the staff of the City of London School for their support and assistance with this study; as well as Gary Griffin, School Second Master, for coordinating pupils and staff, and accommodating the research team on the school premises; and Angelos Sinapis, Takehiro Yamashita, Nino Hirnschall, Ryo Asaoka, Pak Sang Lee, and Edward White for their assistance in running the study.

Supported in part by the Department of Health's NIHR Biomedical Research Centre for Ophthalmology at Moorfields Eye Hospital and UCL Institute of Ophthalmology.

Disclosure: **A. Shah**, None; **S. Low**, None; **D.F. Garway-Heath**, Carl Zeiss Meditec (F); **P. J. Foster**, None; **K. Barton**, None

References

1. Karickhoff JR. Pigmentary dispersion syndrome and pigmentary glaucoma: a new mechanism concept, a new treatment, and a new technique. *Ophthalmic Surg*. 1992;23:269–277.
2. Campbell DG. Pigmentary dispersion and glaucoma. A new theory. *Arch Ophthalmol*. 1979;97:1667–1672.

3. Carassa RG, Bettin P, Fiori M, Brancato R. Nd:YAG laser iridotomy in pigment dispersion syndrome: an ultrasound biomicroscopic study. *Br J Ophthalmol*. 1998;82:150–153.
4. Haargaard B, Jensen PK, Kessing SV, Nissen OI. Exercise and iris concavity in healthy eyes. *Acta Ophthalmol Scand*. 2001; 79:277–282.
5. Saw SM, Chua WH, Gazzard G, Koh D, Tan DT, Stone RA. Eye growth changes in myopic children in Singapore. *Br J Ophthalmol*. 2005;89:1489–1494.
6. Zadnik K, Manny RE, Yu JA, et al. Ocular component data in school children as a function of age and gender. *Optom Vis Sci*. 2003;80:226–236.
7. Williams C, Miller LL, Gazzard G, Saw SM. A comparison of measures of reading and intelligence as risk factors for the development of myopia in a UK cohort of children. *Br J Ophthalmol*. 2008;92:1117–1121.
8. Xiang F, He M, Morgan IG. Annual changes in refractive errors and ocular components before and after the onset of myopia in chinese children. *Ophthalmology*. 2012;119:1478–1484.
9. Hussin HM, Spry PG, Majid MA, Gouws P. Reliability and validity of the partial coherence interferometry for measurement of ocular axial length in children. *Eye (Lond)*. 2006;20: 1021–1024.
10. Kimura S, Hasebe S, Miyata M, Hamasaki I, Ohtsuki H. Axial length measurement using partial coherence interferometry in myopic children: repeatability of the measurement and comparison with refractive components. *Jpn J Ophthalmol*. 2007;51:105–110.
11. Luce DA. Determining in vivo biomechanical properties of the cornea with an ocular response analyzer. *J Cataract Refract Surg*. 2005;31:156–162.
12. Song Y, Congdon N, Li L, et al. Corneal hysteresis and axial length among Chinese secondary school children: the Xichang Pediatric Refractive Error Study (X-PRES) report no. 4. *Am J Ophthalmol*. 2008;145:819–826.
13. Lim L, Gazzard G, Chan YH, et al. Cornea biomechanical characteristics and their correlates with refractive error in Singaporean children. *Invest Ophthalmol Vis Sci*. 2008;49: 3852–3857.
14. Urbaniak GC, Plous S. Research Randomizer. Available at: http://www.randomizer.org/. Accessed November 2009.
15. Moreno-Montanes J, Maldonado MJ, Garcia N, Mendiluce L, Garcia-Gomez PJ, Segui-Gomez M. Reproducibility and clinical relevance of the ocular response analyzer in nonoperated eyes: corneal biomechanical and tonometric implications. *Invest Ophthalmol Vis Sci*. 2008;49:968–974.
16. Luce D. Methodology for corneal compensated IOP and corneal resistance factor for an ocular response analyzer. Available at: http://doclibrary.com/MSC167/PRM/Luce-2006-13559.pdf. Accessed September 2013.
17. Sakata LM, Lavanya R, Friedman DS, et al. Assessment of the scleral spur in anterior segment optical coherence tomography images. *Arch Ophthalmol*. 2008;126:181–185.
18. Pavlin CJ, Harasiewicz K, Foster FS. Ultrasound biomicroscopy of anterior segment structures in normal and glaucomatous eyes. *Am J Ophthalmol*. 1992;113:381–389.
19. Radhakrishnan S, Goldsmith J, Huang D, et al. Comparison of optical coherence tomography and ultrasound biomicroscopy for detection of narrow anterior chamber angles. *Arch Ophthalmol*. 2005;123:1053–1059.
20. Dorairaj S, Oliveira C, Fose AK, et al. Accommodation-induced changes in iris curvature. *Exp Eye Res*. 2008;86:220–225.
21. Bunce C. Correlation, agreement, and Bland-Altman analysis: statistical analysis of method comparison studies. *Am J Ophthalmol*. 2009;148:4–6.
22. Helmholtz H. Ueber die Akkommodation des Auges. *Albrecht von Graefes Archiv für Ophthalmologie*. 1855;2:1–74.
23. Drexler W, Baumgartner A, Findl O, Hitzenberger CK, Fercher AF. Biometric investigation of changes in the anterior eye segment during accommodation. *Vision Res*. 1997;37:2789–2800.
24. Sheppard AL, Evans CJ, Singh KD, Wolffsohn JS, Dunne MC, Davies LN. Three-dimensional magnetic resonance imaging of the phakic crystalline lens during accommodation. *Invest Ophthalmol Vis Sci*. 2011;52:3689–3697.
25. Lord FD, Pathanapitoon K, Mikelberg FS. Keratometry and axial length in pigment dispersion syndrome: a descriptive case-control study. *J Glaucoma*. 2001;10:383–385.
26. Yip LW, Sothornwit N, Berkowitz J, Mikelberg FS. A comparison of interocular differences in patients with pigment dispersion syndrome. *J Glaucoma*. 2009;18:1–5.
27. Ritch R, Steinberger D, Liebmann JM. Prevalence of pigment dispersion syndrome in a population undergoing glaucoma screening. *Am J Ophthalmol*. 1993;115:707–710.
28. Liu S, Li H, Dorairaj S, et al. Assessment of scleral spur visibility with anterior segment optical coherence tomography. *J Glaucoma*. 2010;19:132–135.
29. Kirwan C, O'Keefe M, Lanigan B. Corneal hysteresis and intraocular pressure measurement in children using the reichert ocular response analyzer. *Am J Ophthalmol*. 2006; 142:990–992.
30. Huang Y, Huang C, Li L, et al. Corneal biomechanics, refractive error, and axial length in Chinese primary school children. *Invest Ophthalmol Vis Sci*. 2011;52:4923–4928.
31. Chang PY, Chang SW, Wang JY. Assessment of corneal biomechanical properties and intraocular pressure with the Ocular Response Analyzer in childhood myopia. *Br J Ophthalmol*. 2010;94:877–881.
32. Kotecha A, Elsheikh A, Roberts CR, Zhu H, Garway-Heath DF. Corneal thickness- and age-related biomechanical properties of the cornea measured with the ocular response analyzer. *Invest Ophthalmol Vis Sci*. 2006;47:5337–5347.
33. Hwang HS, Park SK, Kim MS. The biomechanical properties of the cornea and anterior segment parameters. *BMC Ophthalmol*. 2013;13:49.
34. Klingenstein A, Kernt M, Seidensticker F, Kampik A, Hirneiss C. Anterior-segment morphology and corneal biomechanical characteristics in pigmentary glaucoma. *Clin Ophthalmol*. 2014;8:119–126.
35. Scheie HG, Cameron JD. Pigment dispersion syndrome: a clinical study. *Br J Ophthalmol*. 1981;65:264–269.
36. Siddiqui Y, Ten Hulzen RD, Cameron JD, Hodge DO, Johnson DH. What is the risk of developing pigmentary glaucoma from pigment dispersion syndrome? *Am J Ophthalmol*. 2003;135: 794–799.
37. Migliazzo CV, Shaffer RN, Nykin R, Magee S. Long-term analysis of pigmentary dispersion syndrome and pigmentary glaucoma. *Ophthalmology*. 1986;93:1528–1536.
38. Ritch R. A unification hypothesis of pigment dispersion syndrome. *Trans Am Ophthalmol Soc*. 1996;94:381–405, discussion 405–389.
39. Dorairaj SK, Robin A, Shihadeh W, Greenberg S, Liebmann JM, Ritch R. Phenotypic variability of pigment dispersion syndrome in children. *Arch Ophthalmol*. 2007;125:136–138.

Investigative Ophthalmology & Visual Science